N94-25192

An Active Antenna for ELF Magnetic Fields

John F. Sutton, Code 728
Goddard Space Flight Center, NASA
Greenbelt, Maryland 20771

&

Craig Spaniol
Chairman, Dept of Industrial Technology
West Virginia State College
Institute, West Virginia 25112

Introduction

The work of Nikola Tesla, especially that directed toward world-wide electrical energy distribution via excitation of the earth-ionosphere cavity resonances, has stimulated interest in the study of these resonances. Not only are they important for their potential use in the transmission of intelligence and electrical power, they are important because they are an integral part of our natural environment. This paper describes the design of a sensitive, untuned, low noise active antenna which is uniquely suited to modern earth-ionosphere cavity resonance measurements employing fast-Fourier transform techniques for near-real-time data analysis. It capitalizes on a little known field-antenna interaction mechanism.

Recently, the authors made preliminary measurements of the magnetic fields in the earth-ionosphere cavity. [1] During the course of this study, the problem of designing an optimized ELF magnetic field sensor presented itself. The sensor would have to be small, light weight (for portable use), and capable of detecting the 5-50 Hz picoTesla-level signals generated by the natural excitations of the earth-ionosphere cavity resonances. A review of the literature revealed that past researchers had employed extensively very large search coils, both tuned and untuned. Hill and Bostick [2], for example, used coils of 30,000 turns wound on high permeability cores of 1.83 m length, weighing 40 kg! Tuned coils are unsuitable for modern fast-Fourier transform data analysis techniques which require a broad spectrum input. "Untuned" coils connected to high input impedance voltage amplifiers exhibit resonant responses at the resonant frequency determined by the coil inductance and the coil distributed winding capacitance. Also, considered as antennas, they have effective areas equal only to their geometrical areas.

Search coils generate an output voltage having a positive 6dB-per-octave frequency response slope because they are sensitive to the rate of change of the ambient magnetic field. The authors initially employed a zero-input-impedance circuit to eliminate this 6dB-per-octave frequency response slope. (The 6dB-per-octave dependence of the inductive reactance in series with the coil current just balances, by Ohm's law, the effect of the 6dB-per-octave slope of the coil-generated emf.) Sentman [3] mentions that he employed a low-input-impedance preamplifier for the same purpose. The true zero-input-impedance coil-preamplifier combination also has the remarkable property that, because both ends of the coil are maintained at ground potential, the turn-to-turn distributed capacity cannot be charged, and therefore the coil self-resonance is eliminated. Thus, this coil-preamplifier combination provides a uniform frequency response (no self resonance, and no positive 6 Db-per-octave frequency response slope) for arbitrarily large coils out to arbitrarily high frequencies. There is a low frequency pole which is determined by the coil inductance and wire resistance, however.

PRECEDING PAGE BLANK NOT FILMED

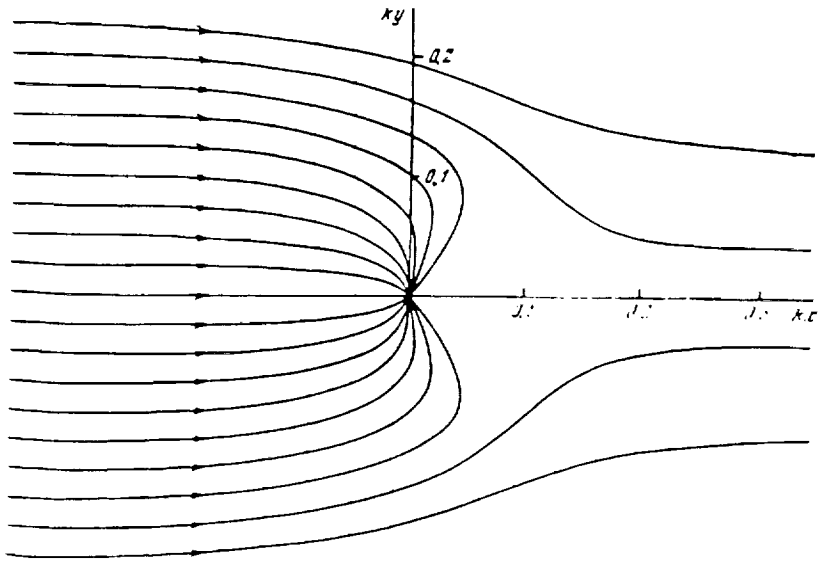

Figure 1. Energy flux lines in the x, y-plane. The dipole located at $x = y = 0$, oscillates in the z direction. Incident (from the left) is a linearly polarized monochromatic plane wave.

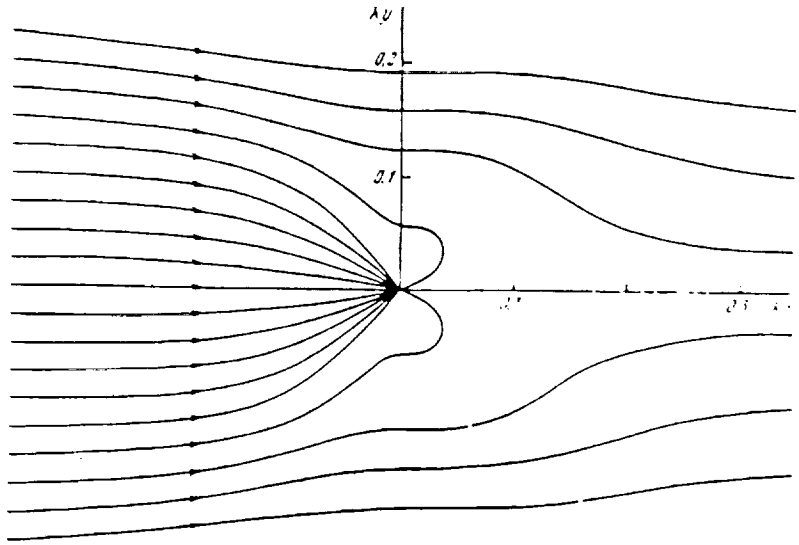

Figure 2. Energy flux lines in the x, y-plane, for the same physical situation as in Figure 1. -- Figures 1 and 2 are from Reference [7].

The untuned coil, zero-input-impedance preamplifier combination can be improved. To see this, we need only compare the functioning of a tuned coil with that of an untuned coil. Aside from the fact that a tuned search-coil antenna has a narrow bandwidth compared to an untuned coil, the differences between a tuned and an untuned antenna are: In the untuned search coil-high input impedance voltage amplifier configuration, essentially no current is permitted to flow in the coil, so there is no magnetic field produced by the coil and, consequently, there is virtually no interaction between the coil and the incoming magnetic field. In the case of the tuned antenna, however, the inductive reactance of the coil and the capacitive reactance of the capacitor cancel each other at the resonance frequency, so that a large current can flow around the tuned circuit. The incoming magnetic field to be detected excites a current in the antenna coil-capacitor circuit, causing this circuit to generate, in turn, a magnetic dipole field. This dipole field, in turn, interacts with the incoming plane wave magnetic field in such a way as to bend the plane wave field lines in the vicinity of the coil. The result is that the Poynting vector lines, which indicate

the direction of energy flow, are bent also. A study of the Poynting vector lines in the vicinity of the coil indicates that the interaction of the dipole field of the tuned coil and the incoming plane wave is such that the antenna circuit absorbs energy from a relatively large portion of the incoming wave front. This phenomenon has been described [4,5,6,7], but is not generally known or appreciated. The interaction results in antennas having effective areas greater than their geometric areas. [8,9] Figures 1 and 2, from Reference [7] are illustrations of the effect. Thus, tuned receiving search-coil antennas can be thought of as dipole field generators in which the dipole field is maintained in phase with the incoming field. To further reduce coil impedance to enhance the dipole interaction, one can employ positive feedback, or regeneration. This technique, which is equivalent to the introduction of negative resistance to cancel the real positive wire resistance of the coil, was employed extensively in the early days of radio. Regenerative antenna circuits fell into disuse at the end of the 1930's because of the interference they generated when allowed to oscillate due to improper adjustment. Isolating buffer circuits between the antenna terminals and the rest of the receiver circuits became the order of the day. Unfortunately, antenna performance suffered as a result of this isolation.

Antenna Design

To improve the performance of untuned antenna coil-preamplifier systems, then, we apply the principle learned from the tuned case: reduce the coil circuit impedance so that coil current will be maximized so that the dipole-plane wave field interaction will be maximized. We begin with the design shown in Figure 3. In this configuration, the coil is attached to the summing junction of an operational amplifier. The summing junction of the operational amplifier is a virtual ground. Thus, the coil is connected between a ground and a virtual ground, and (neglecting wire resistance) there is no circuit impedance other than the self-inductance of the coil, to impede current flow. The self-inductance of the coil presents an impedance which is directly proportional to frequency. Also, Maxwell's equations state that the voltage induced in the coil by the interaction with the incoming field is proportional to the rate of change of the field and therefore has a magnitude which is also directly proportional to frequency. Thus, by Ohm's law, the coil current, and the resulting amplifier output voltage, are independent of frequency.

Negative Resistance Preamplifier

To further improve the untuned coil-preamplifier performance, we can introduce negative resistance into the coil circuit, just as in the tuned case. The combination of the real positive wire resistance (and transformer-coupled resistance effects due to eddy currents in nearby conductors) with the negative resistance produced by the active circuitry results in a coil circuit with as low an effective resistance as desired. One preamplifier configuration which can be employed to accomplish this is shown in Figure 4.

By Ohm's Law, the preamplifier input current is:

$$I = \frac{e_i - e_0}{R_1} \qquad (1)$$

Therefore, the input impedance is:

$$Z_{in} = \frac{e_i}{I_{in}} \qquad (2)$$

or:

$$Z_{in} = \frac{e_i R_1}{e_i - e_o} \tag{3}$$

With the approximation:

$$e_2 = e_1 \tag{4}$$

We have:

$$e_2 = \frac{e_0 K R_2}{R_2 + \frac{1}{jwc}} \tag{5}$$

Where K = fraction of R_2 selected by the potentiometer wiper.

Then, substituting e_0 into Z_{in},

$$Z_{in} = -KR_1 + \frac{1}{jwR_2 C / KR_1} \tag{6}$$

And finally:

$$R_{eff} = -KR_1 \tag{7}$$

$$C_{eff} = \frac{R_2 C}{KR_1} \tag{8}$$

So, we see that the input impedance is a negative resistance-positive capacitance circuit. Putting in the parameter values for our system, we have:

C_{eff} = 0.116 FARAD.

This is effectively a short circuit for reasonable frequencies, so the input impedance, in this approximation, may be considered to be simply a negative resistance. When our search-coil antenna, which has an inductance of +2.15 Henry and a resistance of +49.76 Ohms, is connected to the input of this preamplifier, there is a net circuit resistance of +6.76 Ohms. The inductive reactance of the coil and the capacitance of the active preamplifier form a series resonant circuit having a resonant frequency of 0.3 Hz. The +6.76 Ohm net circuit resistance damps the "Q" of this resonance so that the total active antenna has a flat response, (+/- 1 dB), down to below one Hertz. The response is flat (+/- 1 dB) out to 5 kHz.

Note that, without the positive feedback provided by the circuit of C and R_2, the effective gain of the preamplifier has a low frequency rolloff with a corner frequency determined by the L-R time constant of the coil inductance and the coil resistance. With the parameters of the coil used for these measurements, this corner frequency is 3.68 Hz. With the feedback circuit active, this corner frequency is reduced to 0.5 Hz. Thus, in addition to improving the coupling of the antenna to the incoming plane wave, employing negative resistance feedback greatly extends the low-end flat portion of the antenna-preamplifier frequency response.

Negative Resistance, Negative Inductance, "ZI" Preamplifier

The tuned coil-amplifier antenna circuits of the 1920's had no reactance at the resonant frequency, and by virtue of the regeneration employed, very little circuit resistance, to impede current flow at the resonant frequency. One might ask if it would be possible to obtain the same conditions, i.e., essentially zero circuit impedance, "ZI", in the broad band case. Figure 5 is an example of a circuit which does indeed provide near zero impedance in the untuned case. It is the same circuit as that of Figure 4, with the addition of a capacitance, C_3. After an analysis similar to the analysis of the circuit of Figure 4, the input impedance at the inverting input terminal of the operational amplifier of Figure 5 can be shown to be:

$$Z_{in} = -\frac{R_2 R_4}{R_3} - jwR_2R_4C_3 \qquad (9)$$

With:

$$R_{eff} = -\frac{R_2 R_4}{R_3} \qquad (10)$$

And:

$$L_{eff} = -R_2R_4C_3 \qquad (11)$$

Thus the configuration of Figure 5 results in an input impedance: $Z_{in} = -sCR_2R_4 - R_2R_4/R_3$, which is a negative inductive reactance in series with a negative resistance. With proper choice of the values of R2, R3, R4, and C3, one can adjust the total coil-preamplifier circuit impedance to be an arbitrarily small resistance in series with an arbitrarily small positive inductive reactance. This is the condition for an untuned equivalent to a tuned antenna coil with regeneration, and should produce the maximum possible interaction with the incoming magnetic plain wave.

Another circuit capable of producing the required negative resistance, negative inductance input impedance is given in Figure 6. The input impedance, looking into the noninverting input terminal of the operational amplifier is:

$$Z_{IN} = \frac{E_{IN}}{I_{IN}} \qquad (12)$$

The input current, accordingly, is:

$$I_{IN} = \frac{E_{IN} - E_{OUT}}{R_3} \qquad (13)$$

Now, the output voltage is:

$$E_O = E_{IN} * \left(1 + \frac{Z_2}{R_1}\right) \tag{14}$$

Substituting (13) and (14) into (12) yields:

$$Z_{IN} = \frac{-R_1 R_3}{R_2} - jwC_1 R_1 R_3 \tag{15}$$

Thus, the input impedance is a negative resistance having a value:

$$R_{EFF} = \frac{-R_1 R_3}{R_2} \tag{16}$$

and a negative inductance having a value:

$$L_{EFF} = -C_1 R_1 R_3 \tag{17}$$

Results

We wished to confirm by measurement the principle that antenna current causes an interaction with the signal field such that energy is intercepted from an effective area greater than the antenna geometrical area. Accordingly, a preliminary experimental test was performed on a tuned, regenerative loop antenna-amplifier receiver circuit similar to the standard regenerative receiver circuits of the 1930's. This Q-Multiplier circuit was designed to maximize the antenna coil current consistent with the requirement of circuit gain stability and tuning stability. The circuit diagram for this receiver is given in Figure 7. For comparison purposes, a simple voltage amplifier, Figure 8, was also constructed. This amplifier was designed to have a high input impedance to keep coil current to a minimum so that antenna-field interactions would be minimized. These two amplifiers were used to monitor the 24.3 kHz sideband generated by the U.S. Navy radio station in Cutler, Maine. Cutler is far enough from Washington, D.C. that we can assume that the radiation as received in Washington is, to a good approximation, a perfect plane wave. The coil used for this test consisted of 21 turns of #26 stranded copper wire wound on a 6 1/4 inch diameter form and having an inductance of 116 μH, a resistance of 1.0 Ohms, and a distributed wiring capacitance of approximately 47 pF. This pickup coil was connected in turn to each of the amplifiers, and the output measured with a Hewlett Packard Model 3582A fast-Fourier transform spectrum analyzer. The results were: Voltage Amplifier: -80 dBV, and Q-Multiplier: -40.5 dBV. That is, with the same ambient signal field and the same pickup coil in the same position, the measured output signal of the Q-Multiplier circuit was 39.5 dB greater than that of the simple voltage amplifier.

SPICE analyses (see Appendix) were performed on the two circuits to determine voltage gains. Care was taken to measure the actual component values to better than 1% accuracy to assure accurate analyses. Calculated frequency responses are given in Figs. **9** and **10**. The results were: Voltage Amplifier: +51.6 dB, and Q-Multiplier: +77.9 dB. That is, the

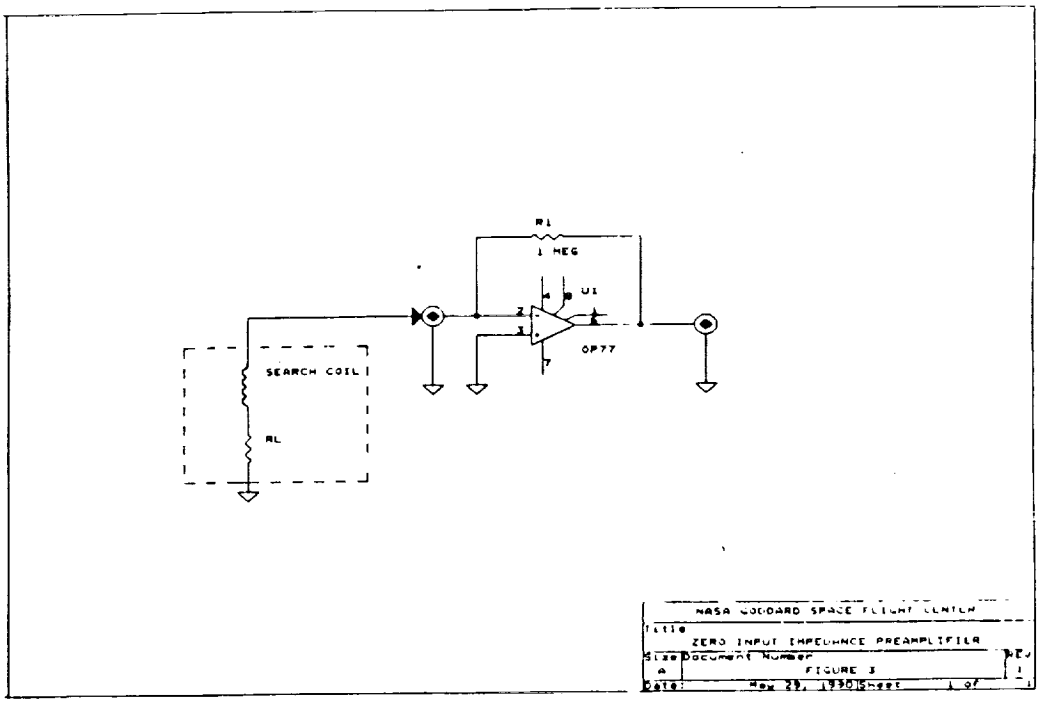

Figure 3. Zero input impedance amplifier.

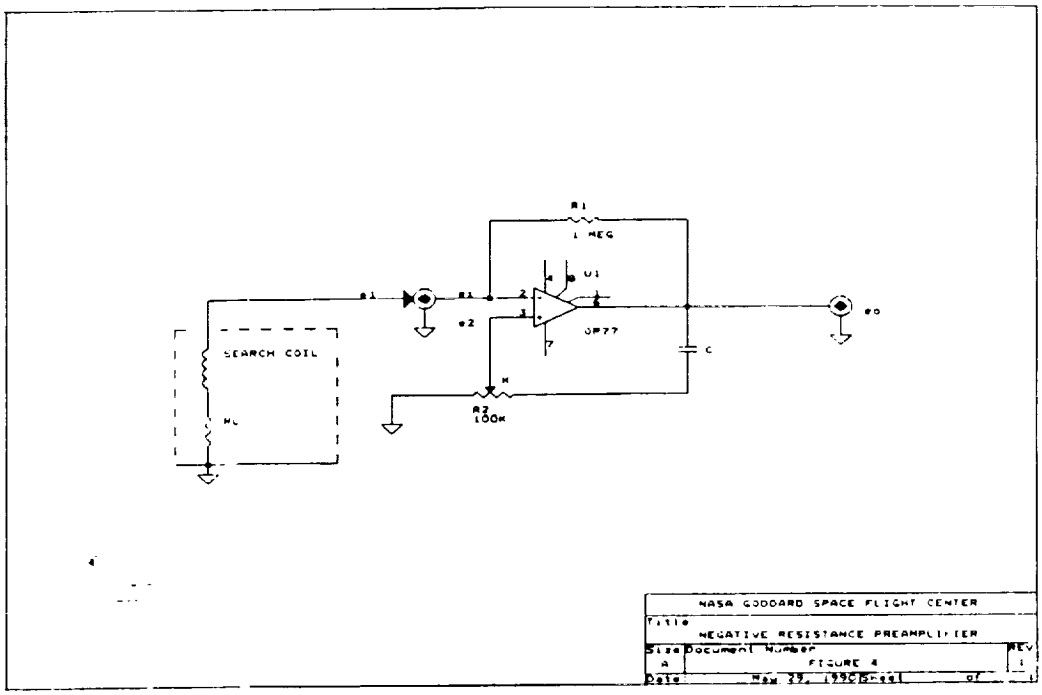

Figure 4. Negative input resistance amplifier.

Q-Multiplier had 26.3 dB more voltage gain than the voltage amplifier. The difference of 39.5dB - 26.3dB = 13.2dB represents an output from the Q-Multiplier circuit which is more than 4.5 times greater than it should be on the basis of circuit voltage gain alone. This means that the effective area of the coil in the Q-Multiplier configuration was over 20 times greater than the geometrical area of the coil and that, therefore, more than 20 times more power was intercepted from the plane wave front, resulting in the 13.2 dB greater output voltage. This is sufficient to demonstrate the principle of plane wave-dipole interaction. The increased output is real signal and therefore represents a real 13.2 dB improvement in signal to amplifier-generated noise ratio.

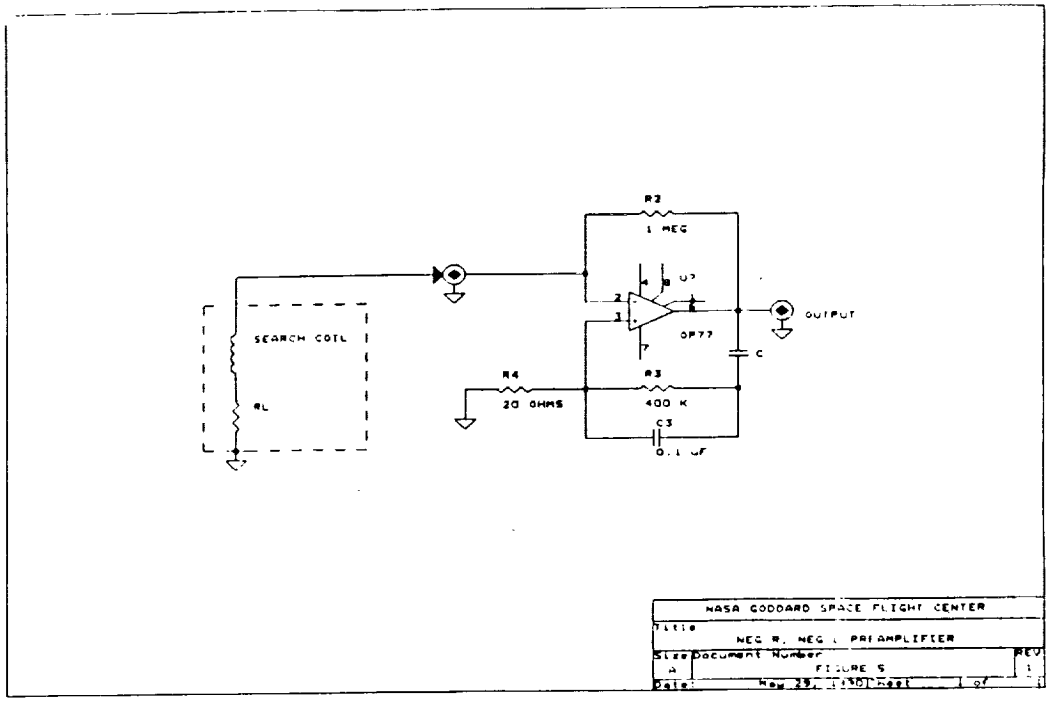

Figure 5. Negative resistance, negative inductance preamplifier.

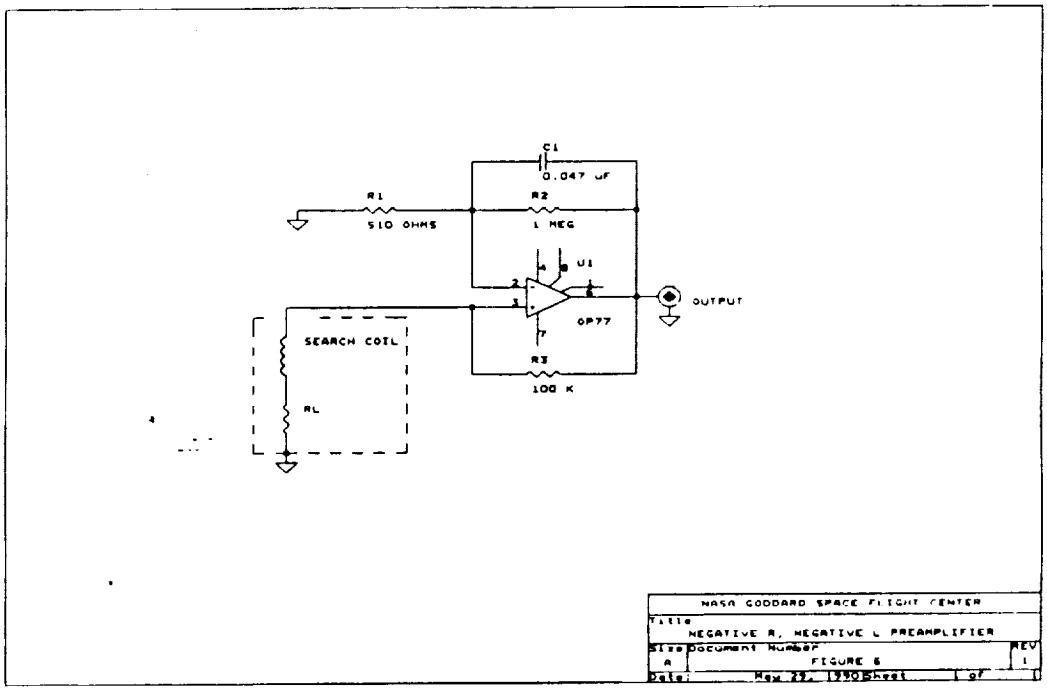

Figure 6. Alternate negative resistance, negative inductance preamplifier.

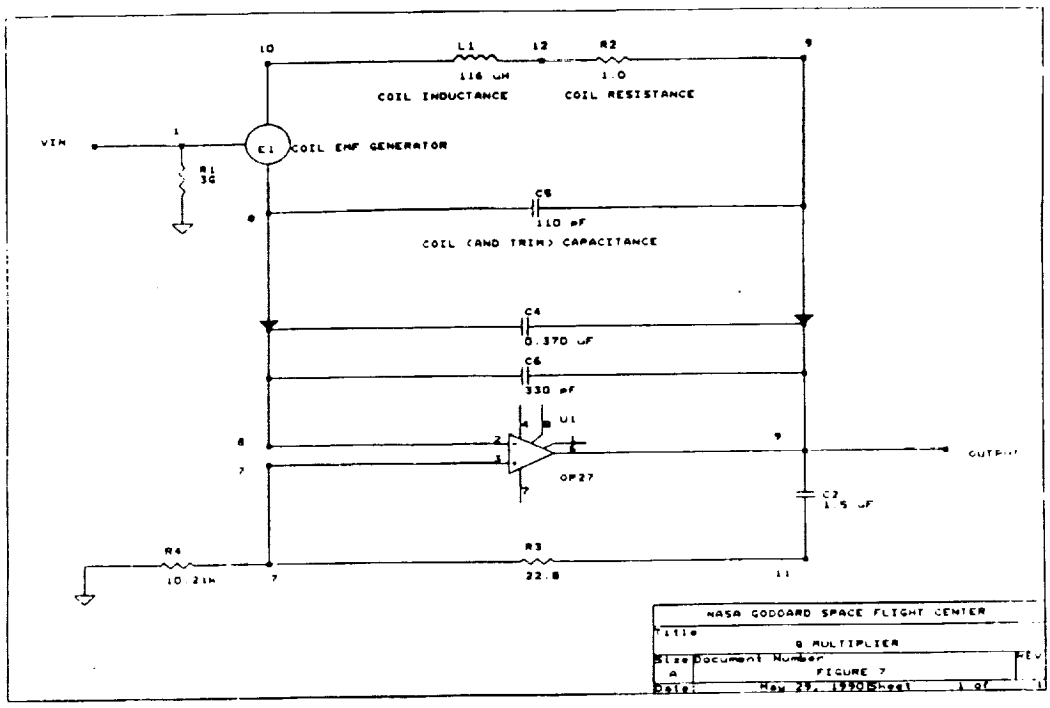

Figure 7. Q-multiplier tuned preamplifier.

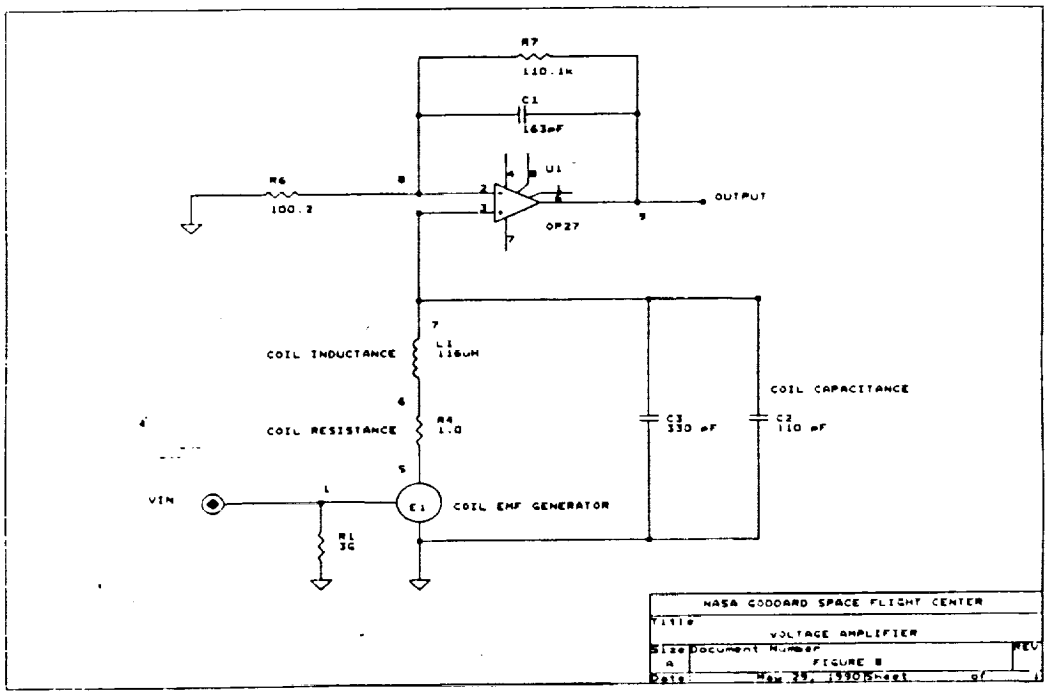

Figure 8. High input impedance voltage preamplifier.

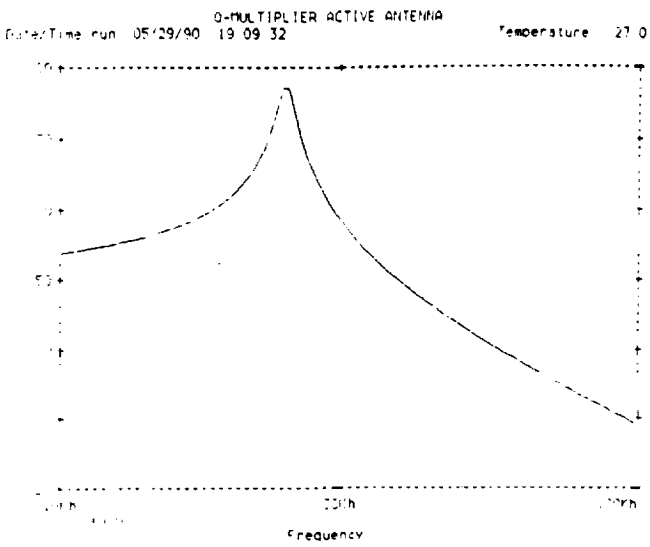

Figure 9. Frequency response of Q-multiplier tuned amplifier.

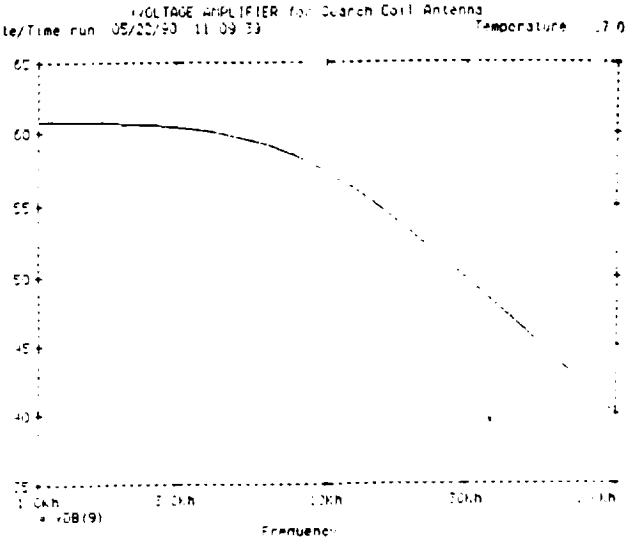

Figure 10. Frequency response of voltage amplifier.

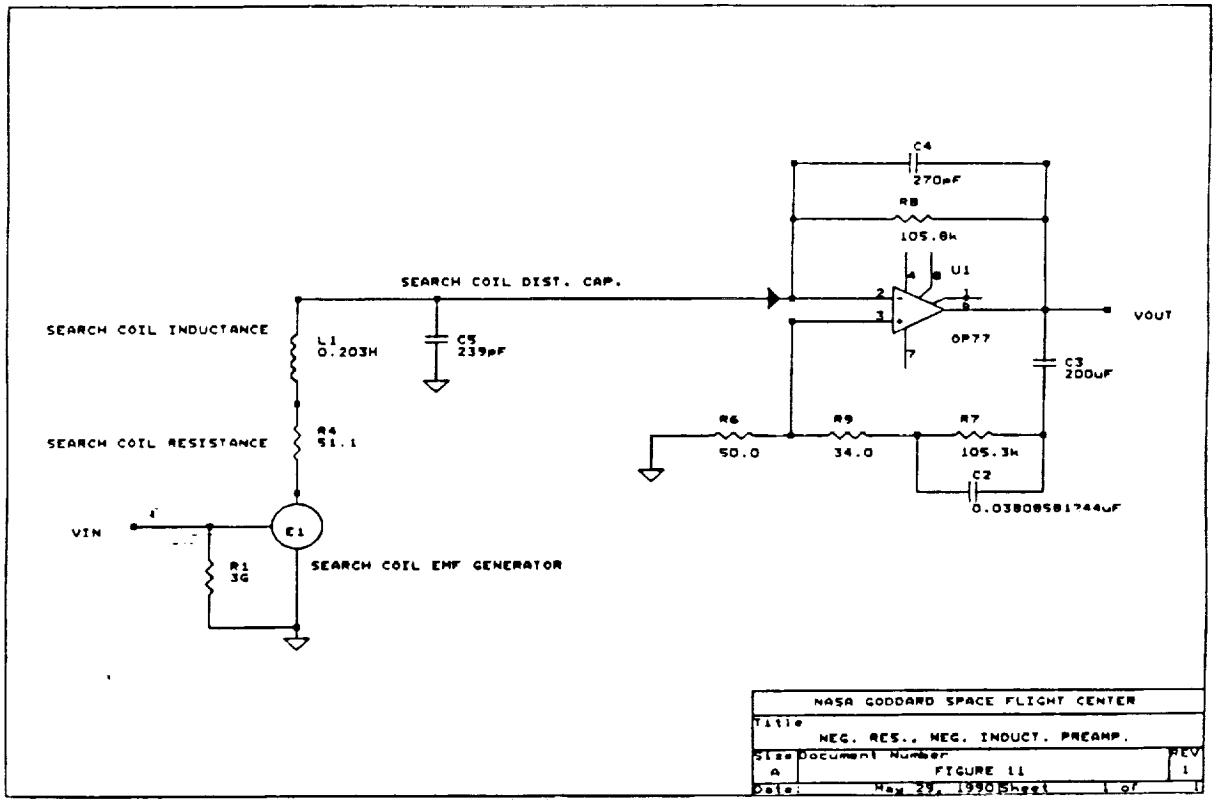

Figure 11. Negative resistance, negative inductance preamplifier.

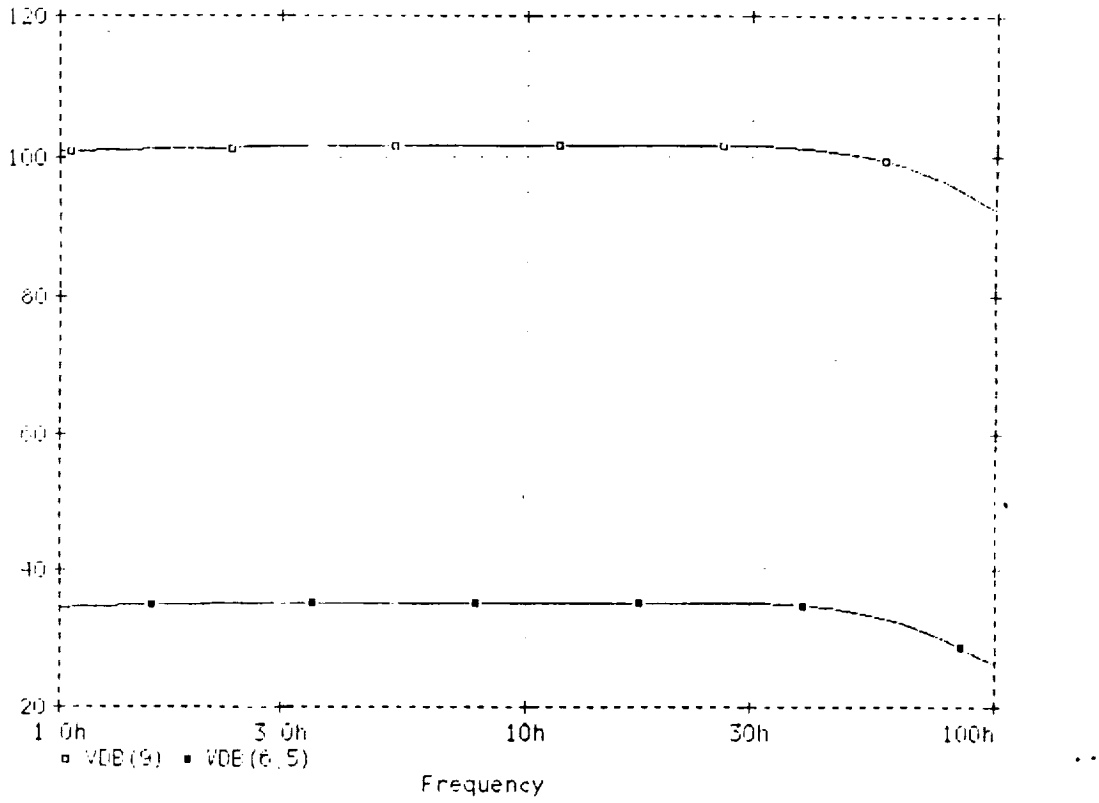

Figure 12. Frequency response of broadband active antenna system.

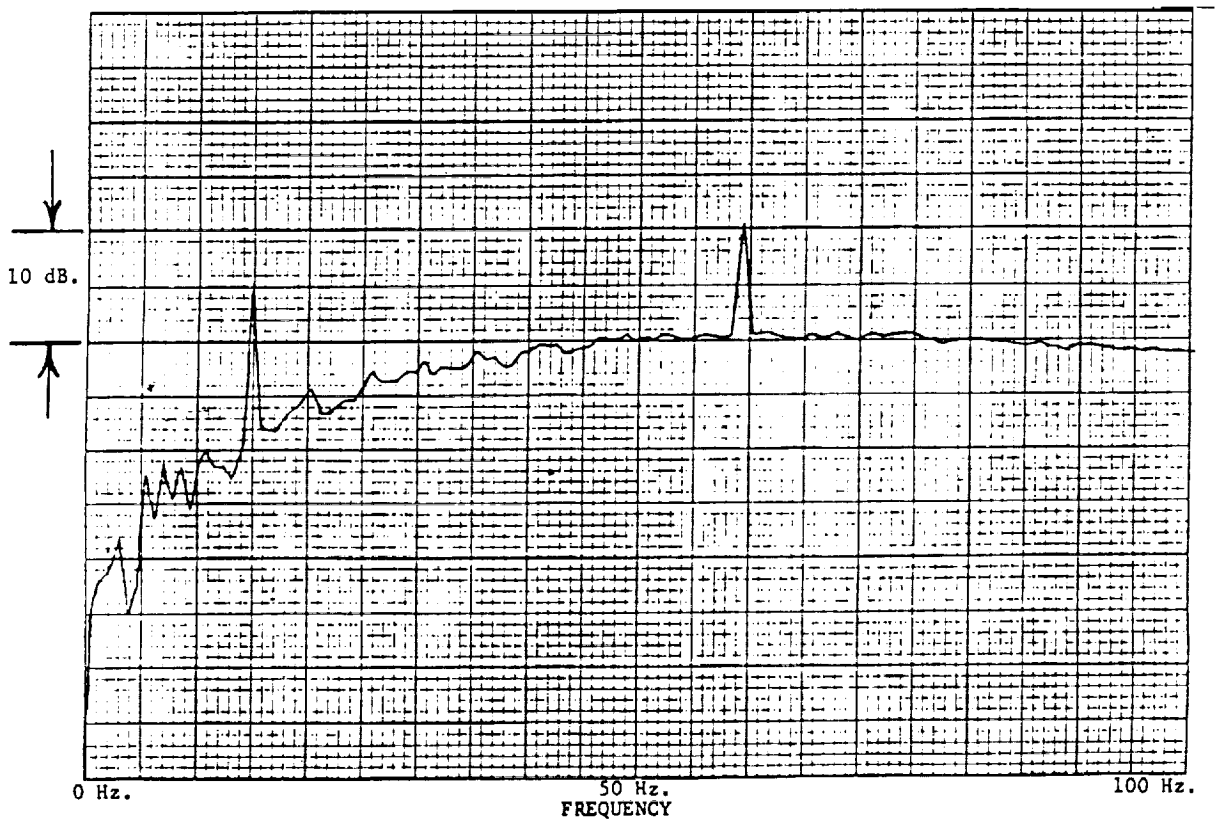

Figure 13. Antenna current verses frequency.

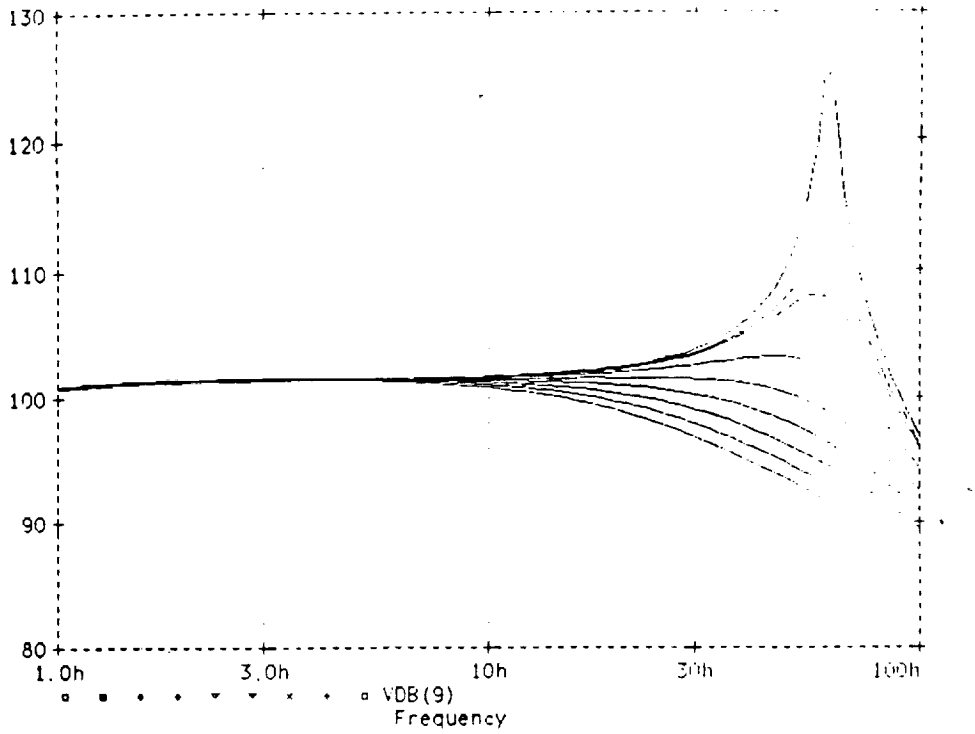

Figure 14. Active antenna gain, C2 stepped in 0.5% increments.

Next, we wished to confirm by measurement, in the broad-band untuned antenna configuration, the same signal enhancement phenomenon observed in the tuned circuit case just described. Accordingly, an active antenna preamplifier having an input impedance consisting of a series combination of a negative resistance and a negative inductance was constructed by combining a coil with the operational amplifier circuit configuration of Figure 11. As is shown in the SPICE analysis, (see Appendix) the amplifier output voltage, VDB(9), has a frequency response, given in Figure 12, which is independent of frequency from 1 Hz to 50 Hz. The voltage drop across the coil resistance, VDB(6,5), is a measure of the coil current and is also found to be independent of frequency. Thus, the SPICE analysis confirms that the total inductive reactance of the coil-preamplifier input circuit is zero from 1 Hz to 50 Hz. The net circuit resistance is the coil resistance of 51.1 Ohms minus the active circuit resistance of -50.24 Ohms, for a net resistance of +0.86 Ohms. The net circuit impedance is therefore solely resistive, and should exhibit a positive 6 dB-per-octave slope when connected to the sensor coil. To confirm this, the sensor coil-preamplifier system was excited by a magnetic field generated by a small coil in series with a 100 Ohm resistor driven by the random voltage generator in the Hewlett Packard model 3582A analyzer. The preamplifier output voltage was then measured as a ratio with the generator voltage. The resulting transfer function, plotted as dB vs. linear frequency, is given in Figure 13. The transfer function does rise at a 6 dB-per octave rate out to 50 Hz., thus qualitatively confirming circuit performance. No direct comparisons between measured output signals and calculated circuit gains could be made as was done in the case of the Q-multiplier. Apparently the SPICE model, in this instance, does not reflect actual circuit performance accurately enough for such comparisons, possibly because of unaccounted-for stray capacitances or inaccuracies inherent in the lumped modeling of the multi-layer solenoid coil. For example, the SPICE analysis indicates that C2 should be tuned to a value of 0.0380858uF, whereas the best experimental value is close to 0.046uF. The curves, Figures 14 and 15, are the calculated coil-active preamplifier gains as a function of the value of the magnitude of C2. Note the dramatic variation in circuit gain as C2 is varied in 0.5% steps. This is due to the critical nulling of the circuit inductive reactance.

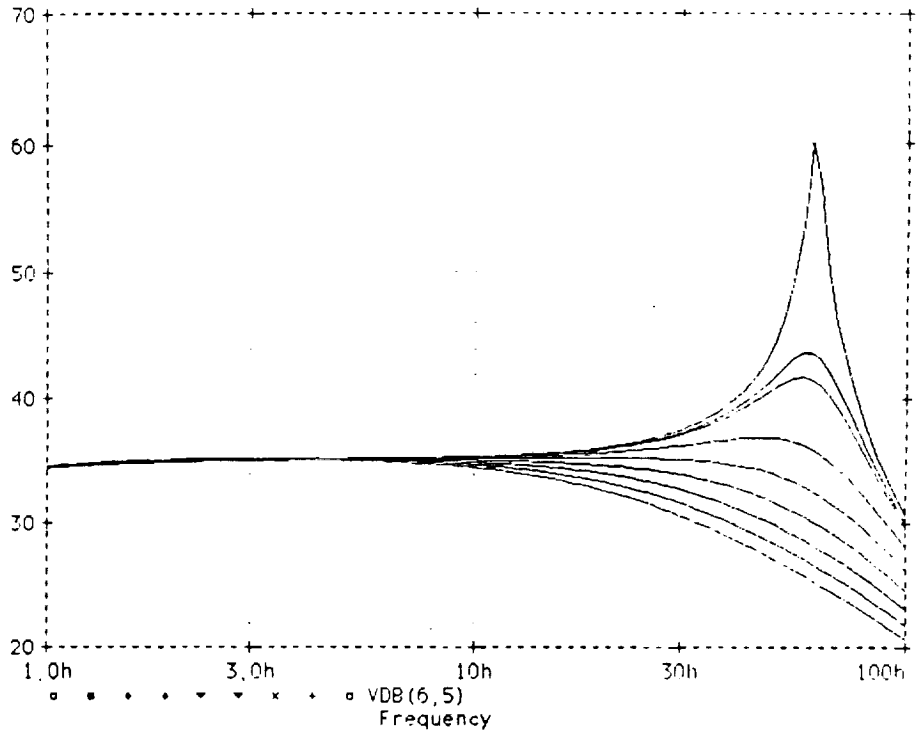

Figure 15. Active antenna current, C2 stepped in 0.5% increments.

To get an idea of the absolute sensitivity of the active antenna system, it was used to detect the field from a small coil of known geometry a known distance from, and coaxial with the sensor, and driven with a known current by a sinusoidal oscillator at various frequencies between 10 Hz and 100 Hz. The amplifier output signal was monitored with the Hewlett Packard model 3582A fast-Fourier transform spectrum analyzer operating in the single channel mode. The calculated value of the field which was just detectable above the noise level was approximately 250 femtoTesla rms. The ambient noise level, typical of a suburban environment, is such that the electronics-noise limit is estimated to be at least one decade below this value, or approximately 25 femtoTesla rms.

Conclusion

We have developed active antenna circuit configurations which can enhance the sensitivity of search coils. The concept of maximizing the antenna-plane wave interaction by eliminating the effect of the resistance and the inductive reactance of the antenna through the application of active circuitry was investigated. Measured and calculated indicators of circuit performance confirm the theoretical dipole-plane wave field interaction in the case of the regenerative tuned circuit. The operation of the broad band, zero impedance antenna circuit has been confirmed qualitatively by experiment. Further refinement of the SPICE computer model will be required to confirm the circuit performance quantitatively.

One might conclude from this study that the ZI configuration is the optimum configuration for a broad band active magnetic field receiving antenna for the ELF band. It could be argued that antenna current cannot be increased beyond that attained with zero circuit impedance. A similar situation existed, however, in the 1920's. Tuned antenna circuits were "pushed" as far as possible with regeneration. Then, a paper [10] titled "Some Recent Developments of Regenerative Circuits", by Edwin H. Armstrong, introduced the concept of superregeneration. The performance of the superregenerative detectors was so superior to that of the regenerative circuits that the latter were all but forgotten. Whether or not the superregeneration concept or some other equally revolutionary concept can be successfully applied to untuned, broad band ELF antennas remains to be seen.

Appendix

Spice Analysis of Active Antenna Circuits

```
******* 01/20/92 ******* PSpice 4.01 - Jan 1989 ******* 12:20:20 *******

VOLTAGE AMPLIFIER

****     CIRCUIT DESCRIPTION

*******************************************************************************


.SUBCKT OP27SMPL 2 3 6
RI 3 2 6E7
CI 3 2 1PF
R2 2 0 3G
R3 3 0 3G
RLP 1 4 1
RO 5 6 60
R4 6 0 3G
CLP 4 0 0.016F
ELP 1 0 2 3 1
EO 5 0 4 0 1.0E6
.ENDS OP27SMPL
X1 8 7 9 OP27SMPL
R1 1 0 3G
R4 5 6 1.0
R6 8 0 100.2
R7 8 9 110.1k
C1 8 9 163pF
C2 0 7 110pF
C3 0 7 330pF
L1 6 7 116uH
E1 5 0 1 0 1
VIN 1 0 AC 1
.OPTIONS NOMOD NOPAGE NOECHO


****     SMALL SIGNAL BIAS SOLUTION       TEMPERATURE =   27.000 DEG C


NODE   VOLTAGE     NODE   VOLTAGE     NODE   VOLTAGE     NODE   VOLTAGE

(    1)    0.0000  (    5)    0.0000  (    6)    0.0000  (    7)    0.0000

(    8)    0.0000  (    9)    0.0000  ( X1.1)    0.0000  ( X1.4)    0.0000

( X1.5)    0.0000


    VOLTAGE SOURCE CURRENTS
    NAME         CURRENT
```

VIN 0.000E+00

TOTAL POWER DISSIPATION 0.00E+00 WATTS

**** AC ANALYSIS TEMPERATURE = 27.000 DEG C

FREQ	VDB(9,0)
1.000E+04	5.380E+01
1.023E+04	5.392E+01
1.047E+04	5.405E+01
1.072E+04	5.417E+01
1.096E+04	5.430E+01
1.122E+04	5.444E+01
1.148E+04	5.458E+01
1.175E+04	5.472E+01
1.202E+04	5.488E+01
1.230E+04	5.503E+01
1.259E+04	5.520E+01
1.288E+04	5.538E+01
1.318E+04	5.556E+01
1.349E+04	5.575E+01
1.380E+04	5.596E+01
1.413E+04	5.618E+01
1.445E+04	5.641E+01
1.479E+04	5.665E+01
1.514E+04	5.691E+01
1.549E+04	5.719E+01
1.585E+04	5.749E+01
1.622E+04	5.781E+01
1.660E+04	5.816E+01
1.698E+04	5.854E+01
1.738E+04	5.895E+01
1.778E+04	5.940E+01
1.820E+04	5.989E+01
1.862E+04	6.044E+01
1.905E+04	6.105E+01
1.950E+04	6.173E+01
1.995E+04	6.250E+01
2.042E+04	6.338E+01
2.089E+04	6.440E+01
2.138E+04	6.561E+01
2.188E+04	6.706E+01
2.239E+04	6.886E+01
2.291E+04	7.114E+01
2.344E+04	7.409E+01
2.399E+04	7.722E+01
2.455E+04	7.714E+01
2.512E+04	7.367E+01
2.570E+04	7.031E+01
2.630E+04	6.761E+01
2.692E+04	6.541E+01
2.754E+04	6.356E+01
2.818E+04	6.196E+01
2.884E+04	6.054E+01
2.951E+04	5.927E+01
3.020E+04	5.811E+01
3.090E+04	5.704E+01
3.162E+04	5.605E+01
3.236E+04	5.511E+01
3.311E+04	5.423E+01
3.388E+04	5.340E+01
3.467E+04	5.260E+01
3.548E+04	5.184E+01
3.631E+04	5.111E+01
3.715E+04	5.041E+01
3.802E+04	4.972E+01
3.890E+04	4.906E+01
3.981E+04	4.842E+01
4.074E+04	4.780E+01
4.169E+04	4.719E+01
4.266E+04	4.659E+01
4.365E+04	4.601E+01
4.467E+04	4.544E+01
4.571E+04	4.488E+01
4.677E+04	4.433E+01
4.786E+04	4.379E+01
4.898E+04	4.326E+01
5.012E+04	4.273E+01
5.129E+04	4.222E+01
5.248E+04	4.171E+01
5.370E+04	4.120E+01
5.495E+04	4.071E+01
5.623E+04	4.021E+01
5.754E+04	3.973E+01
5.888E+04	3.924E+01
6.026E+04	3.876E+01
6.166E+04	3.829E+01
6.310E+04	3.782E+01
6.457E+04	3.735E+01
6.607E+04	3.689E+01
6.761E+04	3.643E+01
6.918E+04	3.597E+01
7.079E+04	3.552E+01
7.244E+04	3.507E+01
7.413E+04	3.462E+01
7.586E+04	3.418E+01
7.762E+04	3.373E+01
7.943E+04	3.329E+01
8.128E+04	3.285E+01
8.318E+04	3.241E+01
8.511E+04	3.198E+01
8.710E+04	3.154E+01
8.913E+04	3.111E+01
9.120E+04	3.068E+01
9.333E+04	3.025E+01
9.550E+04	2.982E+01
9.772E+04	2.940E+01
1.000E+05	2.897E+01

(*)---------- 2.0000E+01 4.0000E+01 6.0000E+01 8.0000E+01 1.0000E+02

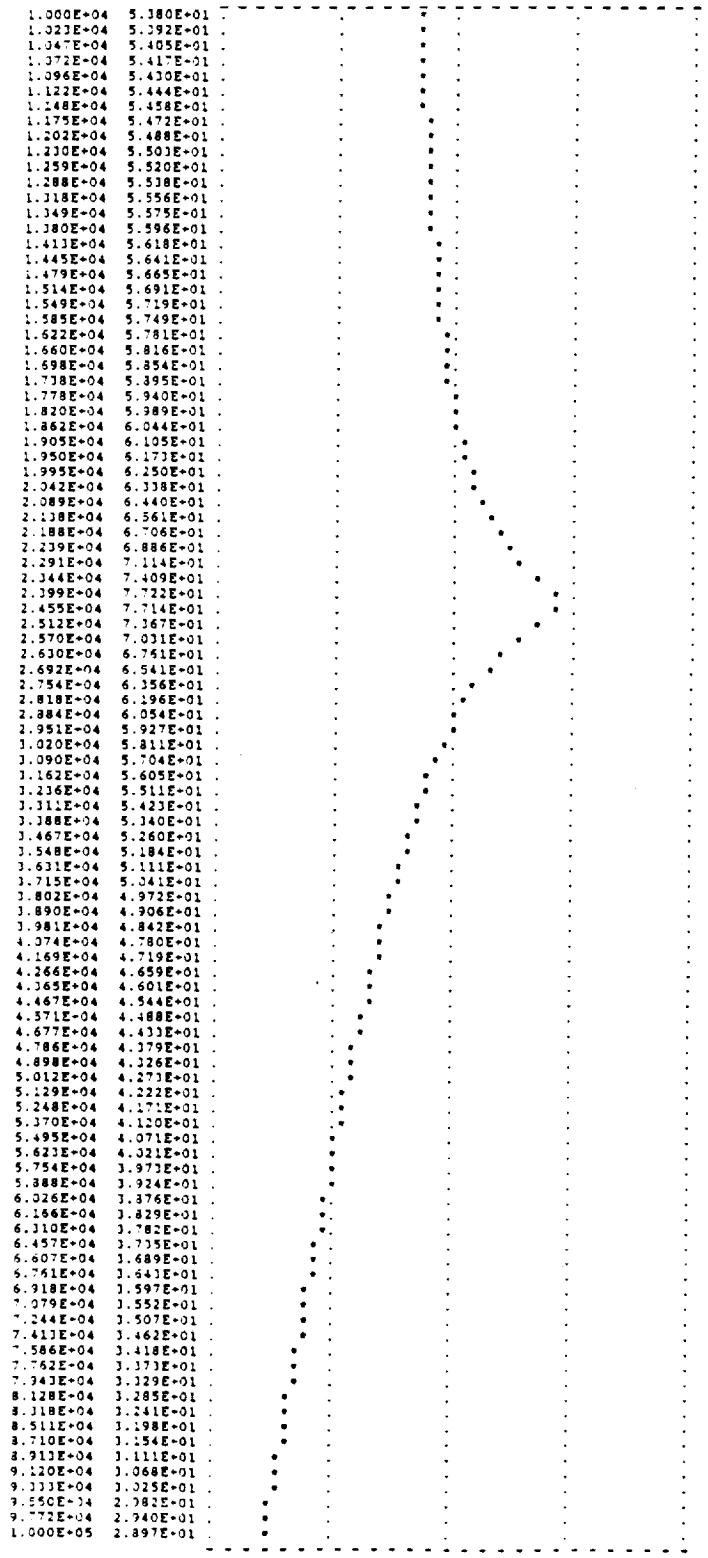

```
******* 01/20/92 ******* PSpice 4.01 - Jan 1989 ******* 12:18:59 *******

Q-MULTIPLIER ACTIVE ANTENNA

****     CIRCUIT DESCRIPTION

**********************************************************************


.SUBCKT OP27SMPL 2 3 6
RI 3 2 6E7
CI 3 2 1PF
R2 2 0 3G
R3 3 0 3G
RLP 1 4 1
RO 5 6 60
R4 6 0 3G
CLP 4 0 0.016F
ELP 1 0 2 3 1
EO 5 0 4 0 1E6
.ENDS OP27SMPL
X1 8 7 9 OP27SMPL
R1 1 0 3G
R2 9 12 1.0
R3 7 11 22.8
R4 7 0 10.21k
L1 10 12 116uH
C2 9 11 1.5uF
C4 9 8 0.370uF
C5 8 9 110pF
C6 8 9 330pF
E1 10 8 1 0 1
VIN 1 0 AC 1
.OPTIONS NOMOD NOPAGE NOECHO


****     SMALL SIGNAL BIAS SOLUTION       TEMPERATURE =   27.000 DEG C

 NODE   VOLTAGE     NODE   VOLTAGE     NODE   VOLTAGE     NODE   VOLTAGE

(    1)    0.0000  (    7)    0.0000  (    8)    0.0000  (    9)    0.0000

(   10)    0.0000  (   11)    0.0000  (   12)    0.0000  ( X1.1)    0.0000

( X1.4)    0.0000  ( X1.5)    0.0000


    VOLTAGE SOURCE CURRENTS
    NAME         CURRENT
```

VIN 0.000E+00

TOTAL POWER DISSIPATION 0.00E+00 WATTS

**** AC ANALYSIS TEMPERATURE = 27.000 DEG C

FREQ	VDB(9,0)
1.000E+03	6.078E+01
1.122E+03	6.077E+01
1.259E+03	6.075E+01
1.413E+03	6.073E+01
1.585E+03	6.070E+01
1.778E+03	6.066E+01
1.995E+03	6.062E+01
2.239E+03	6.057E+01
2.512E+03	6.050E+01
2.818E+03	6.042E+01
3.162E+03	6.032E+01
3.548E+03	6.019E+01
3.981E+03	6.004E+01
4.467E+03	5.985E+01
5.012E+03	5.963E+01
5.623E+03	5.937E+01
6.310E+03	5.905E+01
7.079E+03	5.869E+01
7.943E+03	5.827E+01
8.913E+03	5.780E+01
1.000E+04	5.727E+01
1.122E+04	5.668E+01
1.259E+04	5.604E+01
1.413E+04	5.535E+01
1.585E+04	5.461E+01
1.778E+04	5.383E+01
1.995E+04	5.301E+01
2.239E+04	5.216E+01
2.512E+04	5.129E+01
2.818E+04	5.039E+01
3.162E+04	4.947E+01
3.548E+04	4.854E+01
3.981E+04	4.760E+01
4.467E+04	4.665E+01
5.012E+04	4.569E+01
5.623E+04	4.473E+01
6.310E+04	4.377E+01
7.079E+04	4.280E+01
7.943E+04	4.184E+01
8.913E+04	4.088E+01
1.000E+05	3.993E+01

*)---------- 3.0000E+01 4.0000E+01 5.0000E+01 6.0000E+01 7.0000E+01

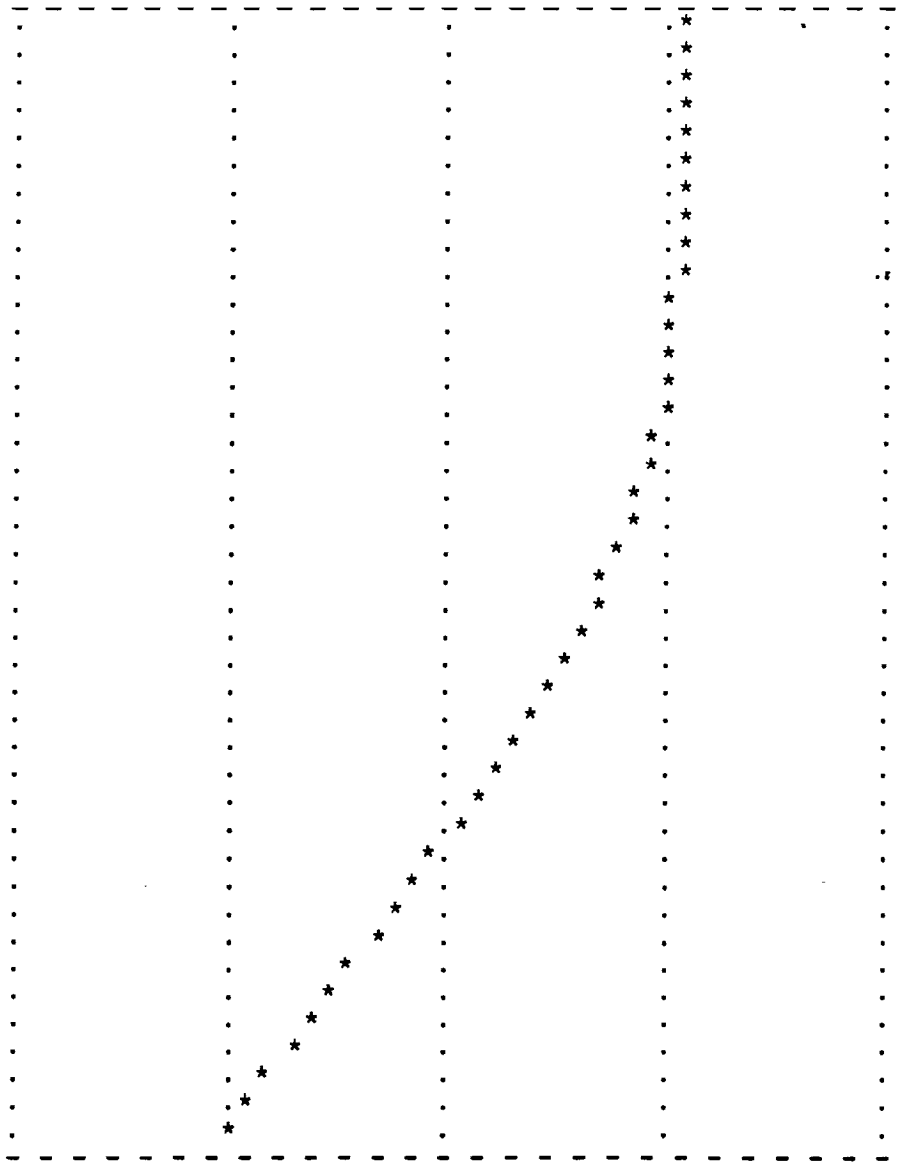

******* 01/20/92 ******* PSpice 4.01 - Jan 1989 ******* 12:26:01 *******

ACTIVE ANTENNA-BROAD BAND

**** CIRCUIT DESCRIPTION

****

```
.SUBCKT OP77SMPL 2 3 6
RI 3 2 4.5E7
CI 3 2 1PF
R2 2 0 400G
R3 3 0 400G
RLP 1 4 1
RO 5 6 60
R4 6 0 3G
CLP 4 0 1.5915F
ELP 1 0 2 3 1
EO 5 0 4 0 1.8E7
.ENDS OP77SMPL
X1 8 7 9 OP77SMPL
R1 1 0 3G
R4 5 6 51.1
R6 7 0 50.0
*R6 7 0 RMOD 48.8
R7 10 11 105.3k
*R7 10 11 RMOD 100k
R8 8 9 105.8k
*R8 8 9 RMOD 100k
R9 7 11 34.0
*R9 7 11 RMOD 51
*R9 ADDED FOR CIRCUIT STABILITY
L1 6 8 0.203H
C2 10 11 0.03808581244uF
*C2 10 11 CMOD 0.03808581244uF
C3 9 10 200uF
*C3 9 10 CMOD 200uF
C4 8 9 270pF
*C4 8 9 CMOD 236pF
*C4 ADDED FOR CIRCUIT STABILITY
C5 0 8 239pF
E1 5 0 1 0 1
VIN 1 0 AC 1
.OPTIONS NOMOD NOPAGE NOECHO
```

**** SMALL SIGNAL BIAS SOLUTION TEMPERATURE = 27.000 DEG C

NODE	VOLTAGE	NODE	VOLTAGE	NODE	VOLTAGE	NODE	VOLTAGE

VOLTAGE SOURCE CURRENTS
NAME CURRENT

VIN 0.000E+00

TOTAL POWER DISSIPATION 0.00E+00 WATTS

**** AC ANALYSIS TEMPERATURE = 27.000 DEG C

LEGEND:

*: VDB(9,0)

FREQ	VDB(9,0)
1.000E+00	1.008E+02
1.122E+00	1.010E+02
1.259E+00	1.011E+02
1.413E+00	1.012E+02
1.585E+00	1.013E+02
1.778E+00	1.013E+02
1.995E+00	1.014E+02
2.239E+00	1.014E+02
2.512E+00	1.014E+02
2.818E+00	1.015E+02
3.162E+00	1.015E+02
3.548E+00	1.015E+02
3.981E+00	1.015E+02
4.467E+00	1.015E+02
5.012E+00	1.015E+02
5.623E+00	1.015E+02
6.310E+00	1.016E+02
7.079E+00	1.016E+02
7.943E+00	1.016E+02
8.913E+00	1.016E+02
1.000E+01	1.016E+02
1.122E+01	1.016E+02
1.259E+01	1.016E+02
1.413E+01	1.016E+02
1.585E+01	1.016E+02
1.778E+01	1.016E+02
1.995E+01	1.016E+02
2.239E+01	1.016E+02
2.512E+01	1.016E+02
2.818E+01	1.015E+02
3.162E+01	1.014E+02
3.548E+01	1.013E+02
3.981E+01	1.011E+02
4.467E+01	1.008E+02
5.012E+01	1.003E+02
5.623E+01	9.954E+01
6.310E+01	9.858E+01
7.079E+01	9.738E+01
7.943E+01	9.595E+01
8.913E+01	9.434E+01
1.000E+02	9.259E+01

(*)---------- 9.0000E+01 9.5000E+01 1.0000E+02 1.0500E+02 1.1000E+02

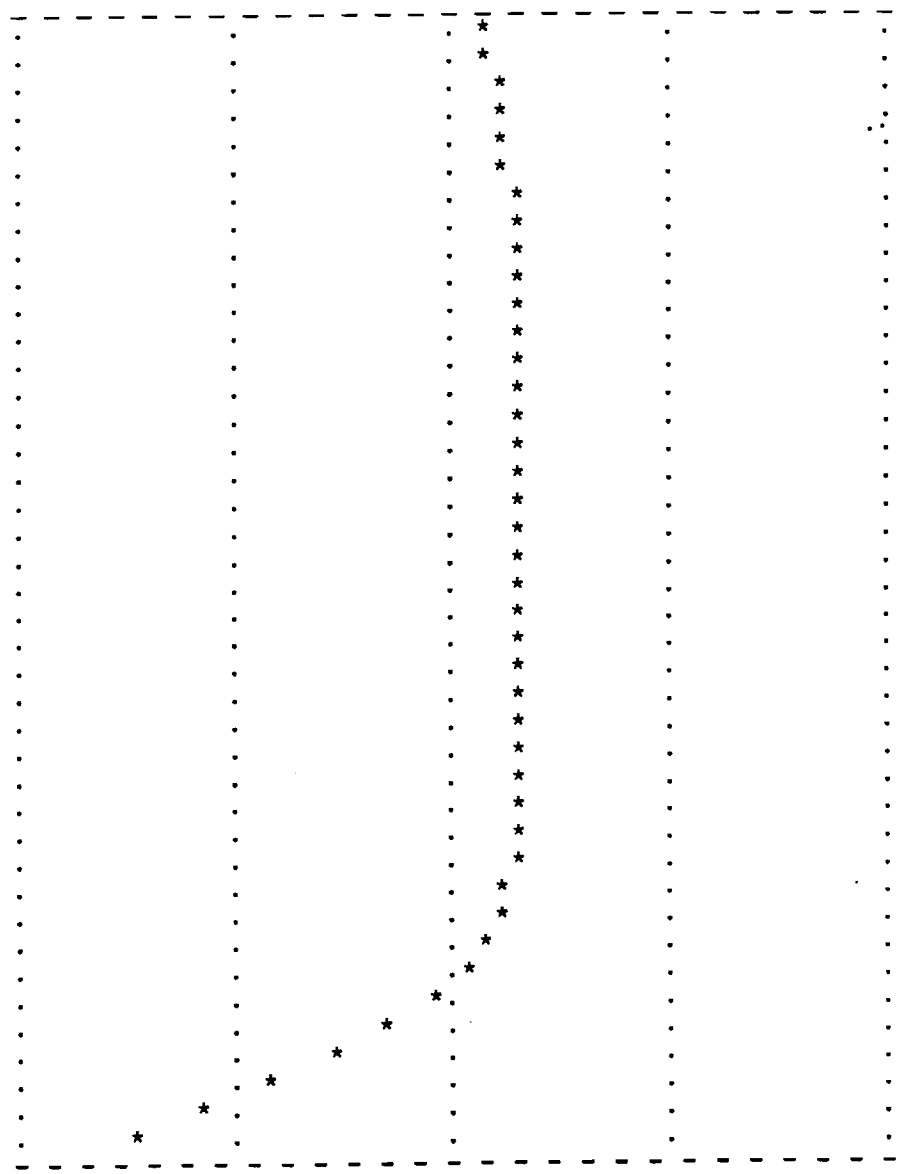

**** AC ANALYSIS TEMPERATURE = 27.000 DEG C

FREQ VDB(6,5)

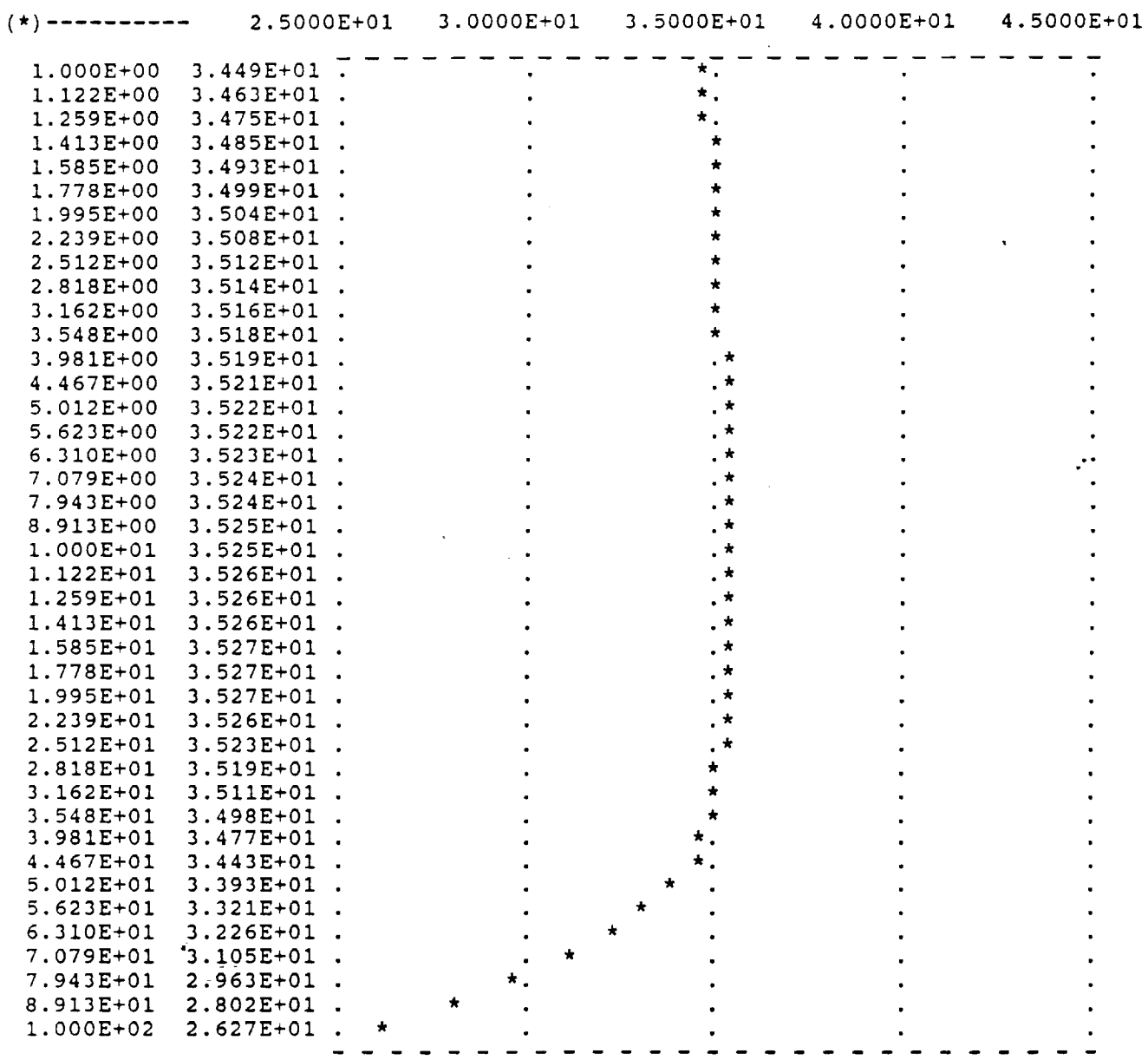

1.000E+00	3.449E+01
1.122E+00	3.463E+01
1.259E+00	3.475E+01
1.413E+00	3.485E+01
1.585E+00	3.493E+01
1.778E+00	3.499E+01
1.995E+00	3.504E+01
2.239E+00	3.508E+01
2.512E+00	3.512E+01
2.818E+00	3.514E+01
3.162E+00	3.516E+01
3.548E+00	3.518E+01
3.981E+00	3.519E+01
4.467E+00	3.521E+01
5.012E+00	3.522E+01
5.623E+00	3.522E+01
6.310E+00	3.523E+01
7.079E+00	3.524E+01
7.943E+00	3.524E+01
8.913E+00	3.525E+01
1.000E+01	3.525E+01
1.122E+01	3.526E+01
1.259E+01	3.526E+01
1.413E+01	3.526E+01
1.585E+01	3.527E+01
1.778E+01	3.527E+01
1.995E+01	3.527E+01
2.239E+01	3.526E+01
2.512E+01	3.523E+01
2.818E+01	3.519E+01
3.162E+01	3.511E+01
3.548E+01	3.498E+01
3.981E+01	3.477E+01
4.467E+01	3.443E+01
5.012E+01	3.393E+01
5.623E+01	3.321E+01
6.310E+01	3.226E+01
7.079E+01	3.105E+01
7.943E+01	2.963E+01
8.913E+01	2.802E+01
1.000E+02	2.627E+01

JOB CONCLUDED

TOTAL JOB TIME 1.15

References

[1] Sutton, John F., and Spaniol, Craig, "A Measurement of the Magnetic Earth-Ionosphere Cavity Resonances in the 3-30 Hz. Range", Proceedings of the International Tesla Society (IEEE), Colorado Springs, Colorado, 1988.

[2] Hill, L.K., and Bostick, F.X., Jr., "Micropulsation Sensors with Laminated Mumetal Cores", Elec. Eng. Res. Lab. Rep. 126, Univ. of Tex., Austin, Tex., 1962.

[3] Sentman, D.D., "Magnetic Elliptical Polarization of Schumann Resonances", Radio Science **22**, No.4, P.595, Jy-Aug, 1987.

[4] Rudenberg, Reinhold, "Der Empfang Electrischer Wellen in der Drahtlosen Telegraphie", Annalen der Physik, Band **25**, P.446, Leipzig, 1908.

[5] Fleming, Ambrose, "On Atoms of Action, Electricity, and Light", Phil. Mag.**14**, P. 591, Jy-Dec., 1932.

[6] Bohren, Craig F., "How Can a Particle Absorb More Than the Light Incident on it?", Am. J. Phys.**51**, No. 4, P.323, April, 1983.

[7] Paul, H., and Fischer, R., "Light Absorption by a Dipole", Sov. Phys. Usp.**26**, No. 10, P. 923, Oct. 1983.

[8] Schelkunoff, S.A., and Friis, H.T., Antennas, Theory and Practice, John Wiley & Sons, Inc., New York, P. 181, 1952.

[9] Williams, H.P., Antenna Theory and Design, Volume Two, Sir Isaac Pitman & Sons, Ltd., London, P.198.

[10] Armstrong, E.H., "Some Recent Developments of Regenerative Circuits", Proc. I.R.E. **10**, P. 244, 1922.

About the Authors

Craig Spaniol, a graduate of Rensselaer Polytechnic Institute and a licensed Professional Engineer, is Chairman of the Department of Industrial Technology at West Virginia State College. He has been involved in expanding educational and industrial opportunities in the Charleston area. Dr. Spaniol is currently conducting NASA supported research on the physical properties of the Earth-ionosphere cavity, and on the fundamental properties of the electron.

John Sutton, a graduate of American University, is a long-time employee of NASA's Goddard Space Flight Center where he has been involved in the design of high performance electronic systems for spacecraft such as COBE and XRS. Dr. Sutton is currently doing research in the areas of the Earth-ionosphere cavity resonances, the infrared absorption of the water molecule, and the physical properties of medical therapy devices.

WEST VIRGINIA STATE COLLEGE
COMMUNITY COLLEGE DIVISION
NASA MEIRF PROJECT
Campus Box 146
P.O. Box 1000
Institute, WV 25112 - 1000